HHS Public Access

Author manuscript

IEEE Trans Ultrason Ferroelectr Freq Control. Author manuscript; available in PMC 2017 November 29.

Published in final edited form as:

IEEE Trans Ultrason Ferroelectr Freq Control. 2017 January ; 64(1): 252–263. doi:10.1109/TUFFC.2016.2619685.

Methods of Generating Submicrometer Phase-Shift Perfluorocarbon Droplets for Applications in Medical Ultrasonography

Paul S. Sheeran [Member, IEEE],
Sunny-brook Research Institute, Sunnybrook Health Sciences Centre, Toronto, ON M4N 3M5, Canada

Naomi Matsuura,
Departments of Medical Imaging and Materials Science and Engineering, University of Toronto, Toronto, ON M5T 1W7, Canada

Mark A. Borden [Member, IEEE],
Department of Mechanical Engineering, University of Colorado Boulder, Boulder, CO 80309 USA

Ross Williams,
Sunny-brook Research Institute, Sunnybrook Health Sciences Centre, Toronto, ON M4N 3M5, Canada

Terry O. Matsunaga,
Department of Medical Imaging, The University of Arizona, Tucson, AZ 85724 USA

Peter N. Burns [Member, IEEE], and
Sunny-brook Research Institute, Sunnybrook Health Sciences Centre, Toronto, ON M4N 3M5, Canada

Paul A. Dayton [Member, IEEE]
Joint Department of Biomedical Engineering, The University of North Carolina at Chapel Hill and North Carolina State University, Chapel Hill, NC 27599 USA

Abstract

Continued advances in the field of ultrasound and ultrasound contrast agents have created new approaches to imaging and medical intervention. Phase-shift perfluorocarbon droplets, which can be vaporized by ultrasound energy to transition from the liquid to the vapor state, are one of the most highly researched alternatives to clinical ultrasound contrast agents (i.e., microbubbles). In this paper, part of a special issue on methods in biomedical ultrasonics, we survey current techniques to prepare ultrasound-activated nanoscale phase-shift perfluorocarbon droplets, including sonication, extrusion, homogenization, microfluidics, and microbubble condensation. We provide example protocols and discuss advantages and limitations of each approach. Finally, we discuss best practice in characterization of this class of contrast agents with respect to size distribution and ultrasound activation.

Paul S. Sheeran and Naomi Matsuura contributed equally to this work.

Index Terms

High-intensity focused ultrasound; medical imaging; therapeutics; ultrasound contrast agents

I. Introduction

Among recent technological advances in medical ultrasonography, the field of ultrasound contrast agents has continued to develop rapidly, both in breadth of applications and continued improvement and specialization of agent formulation techniques. The current clinical standard in contrast-enhanced ultrasonography takes the form of encapsulated gas microspheres, or “microbubbles,” that are designed to circulate intravascularly. The high microbubble echogenicity and nonlinear acoustic response allow for discrimination of the blood compartment from surrounding tissue, which can be used in diagnostic applications spanning echocardiography to cancer [1], [2]. Through the unique acoustic cavitation dynamics at ultrasonic frequencies and modifications in microbubble design, researchers have developed microbubble-based approaches to molecular imaging and therapy that are rapidly approaching the clinic [3]–[6].

In some applications, the size of microbubbles (on the order of 1–5 μm in diameter) and low circulatory persistence (on the order of minutes [7]) are limiting. Phase-shift perfluorocarbon (PFC) droplets are perhaps the most actively researched alternative contrast agent in the field of ultrasound capable of addressing these limitations [8]–[10]. Conceptually, a phase-shift droplet is designed to circulate as a “microbubble precursor” until interaction with the acoustic beam nucleates the liquid core, causing a transition to the vapor state that results in a volumetric expansion on the order of five to six times the original diameter (predicted by ideal gas law relationships [11]). This acoustically triggered transition to a bubble allows for high control over the change in particle density, compressibility, and echogenicity. Although the underlying physics of droplet vaporization are not fully understood, nucleation of the core primarily depends on choice of perfluorocarbon, droplet size, ambient pressure and temperature, the local peak negative pressure of the traveling acoustic wave, and heating from ultrasound absorption [8], [12], [13]. Recent studies have shown that focusing of harmonics within the droplet core can also significantly affect droplet vaporization thresholds [14].

Whereas the useful size range of microbubbles is primarily limited to that which provides both safe passage through the capillary networks and sufficient acoustic response for imaging, phase-shift droplets can be generated across a wider useful size range. Microscale droplets (<10 μm in diameter) may be vaporized to expand and selectively occlude blood flow, enhance thermal ablation, aid drug delivery, or serve as point targets for phase aberration correction [8], [12]. Submicrometer droplets on the order of 100–300 nm may be small enough to exit the “leaky” endothelium of solid tumors [15] and enter into the interstitial space prior to vaporization into micrometer-scale bubbles of ideal size for ultrasound interaction and imaging [16]–[21]. Submicrometer droplets may also have utility for purely intravascular applications such as molecular imaging and measurement of vascular perfusion [22], [23]. For both size regimes, droplets (prior to activation) appear to

provide significantly increased circulation time compared with microbubbles, presumably due to slower dissolution rates and minimized gas exchange/clearance in the lungs [23], [24]. Outside the realm of medical ultrasound, phase-shift droplets may have significant potential in applications such as DNA fragmentation [25] and tissue scaffold patterning [26].

A number of particle generation techniques have been employed since the earliest publications on submicrometer phase-shift droplets. Each method has key advantages and limitations—chiefly depending on which perfluorocarbon is used as the droplet core. In this paper, we first review the governing thermodynamics and design principles surrounding the formulation of phase-shift droplets from volatile compounds. Next, we survey the most common contemporary techniques of producing submicrometer phase-shift droplet emulsions, including example protocols and discussions on best practices and common pitfalls in characterization with the motivation of educating ultrasound researchers new to the techniques and fostering future refinement and standardized protocols.

II. Governing Principles

A. Superheat, Metastability, and Perfluorocarbon Choice

The condition for acoustic droplet vaporization is governed by the thermodynamics and kinetics of the fluorocarbon core. Vaporization occurs when the fluorocarbon molecules acquire sufficient thermal kinetic energy to overcome the attractive intermolecular van der Waals potential energy. From a purely thermodynamics view, this occurs as the system crosses the equilibrium saturation line, which separates the gas and liquid phases as a function of temperature and pressure. Thermodynamics predicts that, for a given temperature (e.g., 37 °C), the droplet vaporizes once the absolute pressure of the acoustic wave drops below the saturation pressure during rarefaction [27]. However, thermodynamics alone fails to predict the existence of superheated droplets (i.e., ones that remain in the liquid state at temperatures and pressures above the saturation curve), as well as the magnitude of the experimentally observed peak negative acoustic pressures required for vaporization of these superheated droplets.

Two theories have been proposed to account for these phenomena in the ultrasound literature. The first theory was given by Rapoport *et al.* [16], who explained the suppression of thermal droplet vaporization as a consequence of Laplace pressure (surface tension at the curved interface), which effectively shifts the equilibrium saturation curve (Antoine's equation) to higher temperatures and lower pressures. Because Laplace pressure scales with inverse droplet radius, the theory explains the observed superheat stability for nanoscale and microscale droplets. However, the theory does not explain all of the observed phenomena. The first and foremost is their stability against phase separation and long shelf life. If the droplets have a significant Laplace pressure, then the emulsion should rapidly coarsen by Ostwald ripening to form larger less thermally stable droplets. A recent theoretical and experimental study showed that fluorocarbon diffusion can be sufficiently rapid to modify the emulsion over the timeframe of just a few minutes [28].

An alternative theory was recently put forth by Mountford *et al.* [29]. This theory explained suppression of droplet vaporization as a consequence of kinetics: the energy barrier for

nucleation of a vapor embryo of critical size. This critical size is the point at which the chemical potential gradient overcomes the Laplace pressure–volume work, and is found as the peak Gibbs free energy when plotted against the embryo radius. Once an embryo of critical size forms, it grows very rapidly to transform the entire liquid phase into a vapor [30]–[32]. For homogeneous nucleation—where the vapor embryo forms in the bulk fluorocarbon liquid phase—the activation energy can be quite large. In contrast, the energy barrier for heterogeneous nucleation (e.g., occurring at surface cracks and impurities) is much reduced and would not stabilize the superheated droplet. The homogeneous nucleation theory does not require a high Laplace pressure in the droplet core, which explains the experimental observation of emulsion stability. The homogeneous nucleation theory also accurately predicts the experimentally observed elevated ambient pressure needed to condense microbubbles [33], where the Laplace pressure theory fails (it predicts a lower pressure). Finally, homogeneous nucleation theory accurately predicts that thermal vaporization must occur at the spinodal (80%–90% of the critical temperature [34]), which marks the boundary of the region where homogeneous states are stable. Thermal vaporization at the spinodal has been observed experimentally [29], [35]. It is important to note that the homogeneous nucleation theory predicts that superheated microscale and nanoscale droplets are in a metastable kinetically trapped state owing to a local minimum in the free energy landscape. The rate of spontaneous vaporization for a droplet population at a given ambient pressure and temperature will depend on multiple aspects of droplet design, including droplet size, encapsulation, and fluorocarbon choice [36].

The implications of homogeneous nucleation theory allow for some practical design principles regarding droplet stability. Rather than rely on the bulk boiling point of the compound as an indication of droplet stability at body temperature, it is instead possible to choose compounds based on the spinodal (approximately 90% of the critical temperature) (Table I). So long as this is well above body temperature, it can be expected that the microscale and nanoscale droplets will remain metastable with minimal spontaneous vaporization. By the same principles surrounding metastability, the choice of perfluorocarbon also impacts vaporization threshold [17], [37], [38]; as the degree of superheat increases, the peak negative pressure required for vaporization decreases. This has been exploited in a number of studies to produce droplets with vaporization thresholds more amenable to use with diagnostic imaging systems. For example, it has been shown that C_3F_8 droplets vaporize at a lower temperature [29], laser fluence [39], and peak negative pressure [23], [38] than for C_4F_{10}, and C_4F_{10} vaporizes at lower peak negative pressures and laser fluence than C_5F_{12}. However, choosing compounds with lower boiling points also comes at the expense of increased emulsion degradation. As molecular weight decreases, the increase in vapor pressure and droplet dissolution can reduce long-term stability [40]. Thus, there is a tradeoff required to produce phase-shift droplets with ideal critical temperature, vaporization pressures, solubility, and biocompatibility. Mixtures of perfluorocarbons can lead to intermediate vaporization thresholds [38], [41]. Unfortunately, it seems that the applicability of mixing highly volatile fluorocarbons (such as C_3F_8 and C_4F_{10}) may be limited by rapid depletion of the species with higher vapor pressure and solubility in systems open to the atmosphere [28]. Further research is needed to determine whether the same effect significantly occurs in mixtures of less volatile fluorocarbons.

Several acoustic vaporization studies have shown that vaporization pressure increases as droplet size is reduced. To the best of our knowledge, this was first reported in [30] for albumin-encapsulated droplets with cores of C_5F_{12}, and has since been observed for other perfluorocarbons and encapsulations [13], [17], [42], [43]. The magnitude of the effect is inconsistent with predictions for the Laplace pressure mechanism alone. For example, Kripfgans *et al.* [30] measured a 3-MHz vaporization threshold increase of approximately 380 kPa for 10-μm diameter droplets compared with 20-μm droplets, while the maximum that can be expected from Laplace pressure for these sizes is on the order of 30 kPa (assuming an unrealistically high surface tension near 70 mN/m). Droplets at the nanoscale have been reported to have vaporization pressures on the order of 2 MPa greater than their microscale counterparts [42], [43], which again contradicts Laplace pressure theory alone.

Alternatively, Shpak *et al.* [14] recently described a super-harmonic focusing effect where transmit pulse harmonics are focused within the droplet by the droplet's curvature, locally increasing peak negative pressure and initiating vaporization. One of the suggestions of the model is that the effect diminishes as droplet size is reduced. With less effective focusing, smaller droplets would require a higher incident pressure for vaporization. This is consistent with [36] that experimentally validates the combination of homogeneous nucleation theory with superharmonic focusing over a broad range of microscale droplet sizes. In another experiment where laser heating rather than acoustic stimulation was used to induce vaporization, the threshold fluence was found to be independent of droplet size, although the droplet size range was somewhat limited in that study [39]. We therefore conclude that homogeneous nucleation is the likely explanation for droplet superheat stability, while superharmonic focusing is likely the explanation for the droplet size effect on acoustic vaporization thresholds.

B. Encapsulation

Since the superheated drops are thermodynamically unstable, kinetically trapped particles in a metastable state, it is critical to "stabilize" them for a time that is sufficiently long for practical use. This is done by choice of the encapsulation, which can stabilize the droplet by inhibiting coalescence, reducing surface tension (reducing Laplace pressure), and retarding diffusion of the fluorocarbon into the surrounding medium. For a lipid encapsulation, one can achieve better stability by simply increasing the cohesion energy through a longer hydrophobic acyl chain length [29], [33]. This strategy, however, must avoid hydrophobic mismatch between the encapsulating lipid species, which inevitably leads to lateral phase separation and poor mechanical stability.

One major advantage of using a lipid is its mechanical flexibility, its ability to form a continuous extended membrane that seals upon itself (self-healing), and the strong adhesion energy to itself (to form bilayers) and to the fluorocarbon/water interface (to form monolayers). These properties allow the lipid monolayer to buckle and fold into bilayer folds upon surface compression, and these folds can then unzip back into the monolayer upon expansion (Fig. 1). Such behavior ensures that the acoustically vaporized bubble is encapsulated and stabilized against dissolution and coalescence. Several studies have experimentally shown that the lipid remains associated with the bubble after vaporization

and continues to influence oscillation dynamics after the bubble has been fully formed [22], [31], [44], [45]. Thus, it is possible to achieve several condensation/vaporization cycles when a lipid is used as the encapsulating material [29]. Note that, while longer lipid acyl chains lead to better stability, they also suppress the rate of vaporization [29], and therefore an optimum should be found.

III. Particle Generation Techniques

A. Sonication

Probe or tip sonication is a general homogenization technique and a common and simple method to produce different types of nanoscale PFC droplets [19], [46], [47]. In this method, a sonication tip is placed directly into a vial containing the components of the droplets (PFC and encapsulation material) and the continuous aqueous phase (typically water or saline). Ultrasound from the tip produces air bubbles that cavitate in the solution, emulsifying the dispersed phase (here, the PFC) within the continuous phase (aqueous solution) with the shell material (e.g., surfactant). Because the final droplet properties, including size and stability, depend on the emulsifier and its interaction with the continuous and dispersed phases, the purity of the emulsion components can affect the final product.

The main benefits of using tip sonication for synthesizing submicrometer droplets are its ease of use (“mix and go”) and the relatively low capital cost of the equipment. Furthermore, since the system is closed with less intrinsic loss in the components of the emulsion during synthesis, relative droplet concentrations can be better quantified compared with other methods that are based on flow techniques where material can be lost during processing. It is also simple to incorporate other agents (e.g., solid nanoparticles or liquid agents [46], [47]) into PFC droplets using tip sonication. This is more difficult using other synthesis methods as even very small aggregates can block the membrane filters used in extrusion or the channels/orifice in microfluidics.

Disadvantages of this technique include the potential destruction of the emulsion components from the high energy input from the probe [48], the erosion of the probe tip that can contaminate the solution and limit translation, and the increased polydispersity of the final droplet population compared with other synthesis methods (Fig. 2).

Another key consideration is that energy input from the probe into the emulsion is very high, and so the local placement of the probe in the solution will have a substantial impact on the final product. The relationship between the sample volume and probe size, the type of tip used, and the placement of the tip in the vessel is extremely important [49]. The vessel must be kept in an ice/water bath during sonication to prevent excess heating, and the tip should be operated in a pulsed mode to prevent vaporization of the droplets during production. It should also be noted that temperature changes can also affect solution viscosity (e.g., of fluorosurfactants) and can also cause temperature-dependent aggregation (e.g., in lipids). Before each sonication procedure, the tip must be visually inspected for any inhomogeneity on its surface—any tip defects will result in increased sloughing of contaminant metal into the solution and poor energy transfer to the solution.

A sample protocol based on the literature is given here [46], [47]. Like all methods, it is easiest to start with a simple formulation [e.g., containing only a single fluorosurfactant as the emulsifier and perfluorocarbon with high thermal stability (e.g., PFH)] to form stable and consistent PFC nanodroplets as a control for new method development. As more experience is gained, more biocompatible compounds and formulations with more volatile perfluorocarbons (e.g., DDFP) can be attempted. For this example, we are using PFH (SynQuest Labs) with the fluorosurfactant Zonyl FSP (Sigma–Aldrich) and a Branson Digital S450D Sonifier (400 W) with a 3-mm microtip.

1. In a narrow glass vessel, dissolve 10 μL FSP in 2 mL ddH_2O. Bath sonicate the mixture for 1 min.
2. Add 60 μL PFH to the mixture.
3. Immerse the vessel in a cold water bath, and sonicate the solution for 5 min, at 10% amplitude (3 W), using a 1-s ON/1-s OFF pulse. Size the droplets.
4. Filter the solution using a sterile <0.45-μm membrane filter to remove large droplets and metal particulates. Use a filter with pores slightly larger than the droplet size. Repeat droplet sizing.
5. Centrifuge the solution to sediment the droplets (e.g., 4000 rpm for 20 min at 4 °C using an Eppendorf 5430 R centrifuge). Draw off and discard the supernatant. If too high a centrifugation speed is selected, the PFC droplets will be destroyed, forming a liquid phase in the bottom of the centrifuge tube.
6. Resuspend the droplets in water/saline to the desired concentration. Droplets should be sized at this stage and evaluated for stability.

B. Extrusion

Extrusion, commonly used for the synthesis of liposomes, can also be simply adapted for the synthesis of PFC droplets [42], [50]–[53]. Membrane extrusion is a gentler way to synthesize PFC droplets compared with sonication. Extrusion typically results in higher monodispersity compared with sonication for a given formulation, with the droplet size controlled by the pore size of the membrane used, ranging from micrometer scale to nanoscale PFC droplets.

However, extrusion is more complex than sonication, and can require substantial formulation-dependent method development. For example, formation of PFC droplets using phospholipids can be difficult due to the preferential formation of liposomes. Also, depending on the phospholipids used and their concentrations, their solubility in the aqueous or PFC phase can lead to aggregate formation that can block the membrane filters. Similarly, the loading of other compounds within the PFC (e.g., nanoparticles or molecular agents) can be challenging.

A method to produce simple fluorosurfactant-stabilized PFH nanodroplets using extrusion is given here. Assumptions are made that the users are familiar with basic extruder operation. For this example, we are using a LIPEXTM 10-mL extruder (Northern Lipids, Inc.) and PFH with the fluoro-surfactant Zonyl FSP. Moving to lower boiling point PFCs (e.g., DDFP)

while using fluorosurfactants is straightforward, but care should be taken to keep the system cooled to below the bulk boiling point of the PFC during extrusion.

1. Combine 2 wt.% of FSP in 4 mL ddH2O to form the continuous phase.
2. Add 0.4 mL of PFC (the dispersed phase) into the continuous phase, and vortex the mixture for 1 min.
3. Load two layers of 1-μm pore size polycarbonate membranes (Nuclepore Track-Etch Membrane, Whatman) in the extruder and load the mixture for extrusion.
4. Extrude the sample ten times (at pressure of ~20 psi).
5. Change the filter to two layers of 0.4-μm pore size membranes and repeat extrusion (approximately five times).
6. Change the filter to two layers of 0.2-μm pore size membranes. Adjust the pressure to ~80 psi. Repeat the extrusion (approximately five times).
7. After extrusion, the sample should be centrifuged and the PFC droplets resuspended in saline or water to the desired concentration as described previously.

Kopechek *et al.* [50] have published a detailed protocol that combines sonication and extrusion to generate submicrometer phospholipid-encapsulated DDFP droplets, which we recommend to the reader.

C. Microbubble Condensation

Generating phase-shift droplets by microbubble condensation first appeared in the research literature in response to the challenge of generating droplets from highly volatile compounds such as decafluorobutane, which exists in the vapor state at room temperature. Initial attempts to produce DFB droplets involved extrusion at temperatures below −2 °C (the boiling point of DFB) [17]. However, the low surface tension of DFB in the liquid state and the high viscosity of the phospholipid solution at these temperatures proved difficult in forming viable submicrometer distributions. As a solution, Sheeran *et al.* [54] proposed instead condensing “precursor” microbubbles with DFB cores into submicrometer droplets by reducing ambient temperature and increasing ambient pressure until the core converts to the liquid state.

This approach yields some significant advantages, including simplicity of generating high-concentration droplet emulsions of volatile compounds (reduced vaporization thresholds compared with droplets of DDFP and PFH) with minimal equipment requirements and the ability to modify and manipulate microbubbles at the microscale prior to condensation [22], [33], [39], [43]. It has more recently been adapted to produce photoacoustic contrast agents [39], [55], and provides a novel opportunity to produce phase-shift droplets directly from commercially available microbubble contrast agents [35]. However, there are some limitations. For research purposes, a well-developed microbubble synthesis protocol is required unless commercial microbubbles—significantly more expensive—are used. As most microbubble distributions are highly polydisperse, producing droplets with narrow size distributions at the nanoscale is relatively difficult, although differential centrifugation can

be utilized to overcome this [56]. While it is relatively simple to incorporate particles, dyes, and targeting ligands into the droplet shell [22], [38], [39], it is difficult to encapsulate particles within the core of the resulting droplet. The volumetric decrease during condensation can produce phospholipid shedding [33], although optimal formulation can mitigate this secondary effect [29]. Finally, many microbubble preparation techniques contain large microbubble outliers that may also be condensed—producing very large droplets that may interfere with intended use *in vivo* unless removed during processing [43].

As microbubble synthesis methods are beyond the scope of this paper, we present an example protocol that assumes a phospholipid-encapsulated DFB microbubble emulsion is already prepared in a glass container (e.g., 3-mL Wheaton vial) with a headspace of DFB vapor and sealed with a rubber septum.

1. Cool a bath of alcohol (e.g., *N*-propanol) to −10 °C with pieces of dry ice and maintain this temperature.
2. Swirl the vial of microbubbles to ensure that it is well mixed. Submerge the vial until the microbubble layer is below the surface of the cooling bath. Continue swirling for 30 s to cool vial contents.
3. Vent the vial by piercing the rubber septum with an 18–21 G syringe needle. This prevents negative pressure from developing inside the vial at the reduced temperature that counteracts condensation.
4. While vented, continue swirling for 1 min 30 s and then remove from the alcohol bath (as needed—see the discussion in the following).
5. To aid condensation, attach syringe or pressure source to venting needle. Submerge vial, continue swirling, and gradually increase headspace pressure until change in vial consistency is observed.
6. Remove the venting needle and store at 4 °C prior to use.

Fig. 3(a) and (b) shows an example of phospholipid-encapsulated DFB microbubbles (following the recipe in [23]) and size distribution (measured by Accusizer 780, Particle Sizing Systems, Santa Barbara, CA, USA) prior to condensation. Note the milky appearance of the microbubble solution and the polydisperse size distribution. Fig. 3(c) and (d) shows the same vial after condensation, accompanied by the sub-micrometer size distribution (measured by NS-500, Malvern Instruments, Westborough, MA, USA). Note the change in translucency and the shift of the distribution peak into the 100–200-nm range. Studies have shown that condensation of the microbubble precursors generally follows ideal gas law expectations and that revaporization of the droplets produces a similar microbubble distribution to the precursor distribution with appropriate experimental conditions [39], [57] (see the discussion for role of secondary effects).

From our experience, some common pitfalls are encountered during microbubble condensation. This method generally works best when the solution can be cooled to below the boiling point of the compound in the microbubble core, causing condensation by temperature alone. For DFB, this means temperatures on the order of −5 °C to −10 °C. The ability to maintain this cooling without freezing the vial components strongly depends on the

composition of the excipient solution (ratio of saline, propylene glycol, glycerol, etc.). For solutions that cannot be cooled to below the compound's boiling point without freezing, it is possible to condense by cooling to the nearest feasible temperature and then increasing the headspace pressure gradually (e.g., 5-psi increments) until condensation is observed. This is the approach used when generating droplets from the highly volatile perfluorocarbon OFP (boiling point = −37 °C) [38].

Condensation of a microbubble can be impeded by both the phospholipid shell and the presence of other species of dissolved gases in the microbubble core [33], [58]. When microbubbles do not condense under the expected conditions, the most common source is compromised perfluorocarbon purity in the microbubble core (e.g., from a poor gas-exchange process). In this case, the microbubbles can usually still be condensed by applying incremental headspace pressure as described above until the phase transition is observed, though it may not produce the same submicrometer emulsion obtained for microbubbles of higher PFC purity.

D. Microfluidics

Monodisperse droplets with coefficient of variation (CV) <5.0% cannot be easily achieved using sonication, extrusion, or microbubble condensation. Microfluidics can produce emulsions with excellent size control and with superior monodispersity compared with other droplet synthesis methods (e.g., sonication, extrusion, or manual or mechanical agitation). However, the formation of nanoscale droplets (i.e., smaller than the minimum dimension of standard microfluidic devices, typically a few micrometers) is more challenging. Unacceptable increases in CV typically occur as the droplet dimensions approach the minimum size that can be generated by the microfluidic system [59]–[61].

Several new microfluidic methods have been introduced to produce monodisperse nanoscale PFC droplets. Microfluidics can directly generate nanoscale droplets in the tip-streaming regime. Martz *et al.* [62] reported production of DDFP (C_5F_{12}) droplets with diameters on the order of 360 nm in this flow regime. In general, producing droplets in the tip-streaming regime is strongly dependent on the capillary number ($0.4 \leq Ca \leq 1.0$), and requires very stable nonfluctuating flows of the dispersed and continuous phases [59]. The smallest size of the droplets that can be obtained through tip streaming is determined by the microfluidic system's viscous forces and surface/interfacial tensions, typically modified through changes in the dimensions and geometries of the microfluidic chip and the properties and flow rates of the fluids [59], [62], [63]. Another direct approach may be through the use of nanofluidic devices [60], [64], but this requires masters fabricated using specialized multilayer nanofabrication techniques.

There have been several indirect methods used to form monodisperse nanoscale PFC droplets from larger monodisperse droplets or bubbles produced using microfluidics. For example, the technique of cosolvent dissolution from cosolvent-infused PFC droplets produced by microfluidics has been used to produce size-reduced PFC droplets approximately five times smaller in diameter than the original microfluidics-produced droplet [65]. An advantage of this technique is the ease of integrating unmodified lipophilic nanoparticles and/or molecular drugs into the PFC core using the cosolvent, which, upon

dissolution, is fully removed leaving behind pure PFC nanodroplets containing the drugs locked within their cores [65], [66].

Another indirect method to produce monodisperse ultra-small PFC droplets uses the condensation of monodisperse precursor bubbles generated using a microfluidic device operating at temperatures higher than the boiling point of the droplet material [67]. Since the condensation of bubbles is limited by the density difference between the gas and liquid phases of the droplet material, this technique is limited to the formation of final droplets that are approximately five times smaller in diameter than the precursor PFC bubbles. The combination of condensation and dissolution of cosolvent-infused bubbles generated by microfluidics has been shown to produce monodisperse PFC droplets substantially smaller in diameter than what can be achieved using either the condensation or dissolution process alone (~24 times smaller in diameter than the precursor droplets) [68], which is promising for the production of monodisperse nanoscale PFC droplets <200 nm in size. It has been shown that monodisperse PFC droplets can be converted to monodisperse bubbles after exposure to high-pressure ultrasound (Fig. 4) [68].

Although no other emulsification method can achieve superior PFC droplet monodispersity compared with microfluidics, the major limitation of microfluidics (besides the difficulty in generating submicrometer droplets/bubbles) is its relatively low production yield (typically $<10^4$–10^6 droplets/s). Generating enough droplets for effective evaluation *in vitro* and *in vivo* requires an extremely stable system and many hours of generation time. Furthermore, microfluidics requires relatively specialized equipment and expertise that could make this method out of reach for novice users.

As a starting point for the novice user, it is recommended that first larger microdroplets are made using microfluidics with a relatively large orifice and a higher boiling point PFC (e.g., PFH) emulsified with a fluorosurfactant. Once this general technique has been perfected, nanoscale droplets can be made by adapting the techniques as introduced above. This example protocol describes the generation of microdroplets with microfluidic flow-focusing method using a three-inlet microfluidic device design in [67]–[69]. Here, the continuous aqueous phase “pinches off” the central fluid of perfluorohexane (dispersed phase) to form droplets. For this example, we are using PFH with the fluorosurfactant Zonyl FSP and Pluronic F-68 (Sigma–Aldrich) to directly produce stable microscale monodisperse perfluorocarbon droplets.

1. Combine 0.5 wt% FSP, 1 wt% F-68, 60 wt% glycerol, and 38.5 wt% ddH_2O to form the continuous phase.
2. With a 10-mL syringe, take 10 mL of the continuous phase solution made in Step 1, and connect the syringe to the port for the continuous phase of the microfluidic chip using polytetrafluoroethylene tubing.
3. With a 1-mL syringe, take 1 mL of PFH and connect it to the port for dispersed phase of the microfluidic chip using polytetrafluoroethylene tubing.
4. Using two syringe pumps, inject the continuous phase in the 10-mL syringe at 1 mL/h and the dispersed phase in the 1-mL syringe at 0.1 mL/h.

5. Wait for 5–10 min for the droplets to start generating.
6. Observe droplet generation at the microfluidic device orifice under an inverted microscope (10x objective) coupled to a high-speed charge-coupled device camera. If the droplet generation is too fast to observe (~400/s) during generation at the orifice, it may instead be viewed more clearly at the collection port.
7. Once it is confirmed that stable microdroplet generation has been established, the microdroplets can be collected by connecting the outlet port to a glass vial with polytetrafluoroethylene tubing.
8. To control droplet generation size, adjust the flow rates of the continuous and dispersed phases. Ensure that the system is equilibrated for 5–10 min after each change of flow rate.

E. Homogenization/Microfluidization

Beginning with some of the earliest reports on submicrometer perfluorocarbon droplets as contrast agents [70], [71] and submicrometer phase-shift droplets [13], [18], [41], researchers have relied on commercial homogenization/microfluidization systems to reduce particle size into the nanoscale. In general, these emulsification products operate by passing the sample through a network of microfluidic channels at high pressure, exposing the sample to high shear rates that break up and reform particles into smaller size distributions. Typically, the process is repeated for several passes to gradually refine the sample distribution. Care must be taken to control the temperature at the system output (commonly with ice-cooled water) to minimize evaporation of the compounds being homogenized. This approach naturally produces a bubbly solution, and the droplets can be separated from the bubbles through techniques such as centrifugation or flotation [70]. In the literature, this approach has been used to produce submicrometer perfluorocarbon droplets composed of PFH and DDFP, but has not, to the best of our knowledge, been applied to lower boiling point compounds.

For phase-shift droplets, the size distribution produced will significantly depend on the homogenizer used (varying geometry and system design with each manufacturer), and so protocols may change significantly across products. As an example protocol, we refer the reader to [70], in which PFH droplets of varying size were produced by homogenization. Reznik *et al.* [18] modified this protocol to produce DDFP droplet emulsions with a mean diameter of 405 nm.

IV. Characterization of Submicrometer Phase-Shift Droplets

A. Particle Sizing and Concentration

Characterization of submicrometer particles is complicated by the fact that the primary distribution exists near or below brightfield resolution limits of microscopy. Similarly, a number of products are available to simultaneously characterize both size and concentration of particles at the microscale (e.g., Coulter counters), but the standard approach to sizing at the nanoscale [dynamic light scattering (DLS)] does not measure concentration and only estimates the true particle distribution indirectly (by extrapolation from scattering intensity).

As such, care must be taken to follow best practice procedures in sample preparation and characterization.

When using instruments that characterize submicrometer distributions by DLS (e.g., Malvern ZetaSizer), we recommend following the guidelines set by the Nanotechnology Characterization Laboratory [72], which comprehensively covers techniques to best characterize samples. While too extensive to reproduce in full, here we mention a few points pertinent to characterizing volatile perfluorocarbon droplets from that guideline as well as from our experience.

1. Samples should be measured across a range of concentrations (serial dilution) and for many repetitions to determine stability in the sizing results. Poor repeatability can result from the particle concentration being either too high (multiple-scattering events) or too low (low signal to noise). Highly polydisperse emulsions can also introduce variability in sizing results, and so a higher number of repetitions and averages should be considered with greater polydispersity.
2. The native measurement in DLS is an intensity distribution. To convert to number distribution with reasonable accuracy, a refractive index within 0.5% of the true value is required. This value is known for many compounds, but there is some inherent uncertainty for perfluorocarbons measured near or above their boiling point (e.g., DFB droplets measured by DLS as 4 °C). Although intensity-weighted distributions overemphasize the large sample content, they should be considered the most trustworthy and displayed alongside extrapolated measurements such as number-weighted or volume-weighted.
3. Many preparations of phase-shift droplets result in polydisperse emulsions, containing both very small (<100 nm) and very large droplets (>500 nm). As particle sizes approach the microscale, sedimentation may occur over the course of several DLS measurements. Comparisons in size for the same sample over long periods of time should be done only if the sample is mixed between measurements.

Because DLS cannot provide estimations of sample concentration, the most common approach is to assume the particle generation technique produces no loss in the volume of PFC used. Combining the known PFC volume with the measured average particle diameter provides a straightforward method of estimating particle concentration [41], [42], [70]. How accurate the “no loss” assumption is will highly depend on the specific particle generation technique and operating conditions chosen. A relatively new generation of particle sizing instruments based on sensitivity to single nanoparticles may circumvent some of the issues described above and provide a new standard of measurement in the future by providing direct number-weighted size along with concentration [73], [74].

In general, submicrometer particle sizing should always be coupled with microscale sizing (e.g., Coulter counters) and/or brightfield microscopy (40–100X magnification) to ensure that large outliers or aggregates beyond the sensitivity of the submicrometer sizer that may interfere with results are not present.

B. Ultrasound Characterization

Droplet vaporization by an ultrasonic pulse is an inherently probabilistic process, and so it would seem intuitive to maximize the likelihood of vaporization using long acoustic pulses at pressures well above the vaporization threshold (but low enough to minimize unwanted bioeffects). The success of this approach likely depends on the intended use of the droplets. For applications where droplets are used to achieve a secondary goal (such as drug delivery or enhancing ablation), or when bubbles produced by vaporization are expected to recondense shortly after the pulse ends (i.e., the droplets are below the equilibrium saturation curve at ambient conditions) [75], this is likely correct. However, when the intent is to create stable bubbles for continuing ultrasound interaction (e.g., imaging) that survive after the pulse ends, repetitive and/or long pulses can change the expected bubble distribution adversely. Studies have shown that small bubbles are selectively destroyed with continuing vaporization pulses, while large bubbles tend to fuse, gradually shifting the bubble distribution toward a larger mean diameter or reducing the total contrast provided [43], [45], [57], [76]. For submicrometer droplet emulsions, which produce bubbles of sizes that are highly responsive to ultrasound imaging frequencies, it may be the case that short acoustic pulses/vaporization sequences are required to minimize unintended microbubble destruction and maximize the resulting contrast. Thus, when stable bubble production is desired, we recommend initial characterization with the shortest acoustic pulse lengths and least number of repetitions possible in order to establish vaporization trends. These trends obtained from short acoustic exposures can then be compared with the results obtained from longer duration exposures that are likely to contain more of the secondary effects described above.

Similar to the sizing considerations in Section IV-A, it is important to assess the impact of distribution outliers on the acoustic performance of the droplet emulsion. It has been reported by multiple groups that vaporization thresholds are reduced as droplet size increases [16], [17], [30]. This is likely due to a number of combined effects, such as decreased Laplace pressure, increased superharmonic focusing, and increased probability of nucleation in the larger volume. Recent studies have shown that large outlier content can greatly skew the measured vaporization threshold and significantly alter *in vivo* performance from that desired [43], [77] (Fig. 5). For the purposes of *in vitro* therapeutic investigations, these outliers may actually dominate the measured effect. Finally, it has been shown that some measurements of droplet activation do not linearly scale with droplet concentration [78]. Therefore, in concert with the sizing practices described in the previous section, we recommend that ultrasound characterization of submicrometer phase-shift droplets should be performed across a range of concentrations that include high dilutions as well as compared against samples filtered to remove microscale content.

V. Conclusion

As highly dynamic agents capable of being activated by externally applied ultrasound, phase-shift droplets provide unique opportunities in the imaging and treatment of disease. We have surveyed in this paper the most commonly reported methods of producing nanoscale phase-shift droplets and have provided example protocols toward the goal of

establishing best practices in the research community. Each method described here has inherent advantages and disadvantages, and the best approach is likely to depend on the application being pursued.

Acknowledgments

This work was supported in part by the Canadian Institutes of Health Research under Grant MOP119346, in part by the Ontario Institute for Cancer Research, in part by the Ontario Research Fund–Research Excellence Program and the Early Researcher Award under Grant ER14-10-178, in part by the Prostate Cancer Canada Movember Foundation under Grant D2014-7, in part by the Fight Against Cancer Innovation Trust, in part by the Canadian Cancer Society under Grant 703909, in part by the NSERC Discovery Grants Program under Grant RGPIN-2015-05835, in part by the Focused Ultrasound Foundation, in part by the National Science Foundation under Grant DMR1122383 and Grant NIH R21EB01174, and in part by the Carolina Center for Cancer Nanotechnology Excellence. The work of P. S. Sheeran was supported by the Banting Postdoctoral Fellowship, Canadian Institutes of Health Research.

P. S. Sheeran would like to thank C. Arena, K. Yoo, and W. Walker for assistance with gathering sizing data presented here. N. Matsuura would like to thank M. Seo, I. Gorelikov, Y. Gao, and Y. Xiang for testing the sonication, extrusion, and microfluidic protocols presented here.

References

1. Wilson SR, Burns PN. Microbubble-enhanced US in body imaging: What role? Radiology. 2010; 257(1):24–39. [PubMed: 20851938]
2. Ferrara K, Pollard R, Borden M. Ultrasound microbubble contrast agents: Fundamentals and application to gene and drug delivery. J Biomed Eng. Aug.2007 9:415–447.
3. Hernot S, Klibanov AL. Microbubbles in ultrasound-triggered drug and gene delivery. Adv Drug Del Rev. Jun; 2008 60(10):1153–1166.
4. Gessner R, Dayton PA. Advances in molecular imaging with ultrasound. Mol Imag. 2010; 9(3):117–127.
5. Martin KH, Dayton PA. Current status and prospects for microbubbles in ultrasound theranostics. Wiley Interdiscip Rev Nanomed Nanobiotechnol. Aug; 2013 5(4):329–345. [PubMed: 23504911]
6. Hynynen K. Ultrasound for drug and gene delivery to the brain. Adv Drug Del Rev. Jun; 2008 60(10):1209–1217.
7. Landmark KE, Johansen PW, Johnson JA, Johansen B, Uran S, Skotland T. Pharmacokinetics of perfluorobutane following intravenous bolus injection and continuous infusion of sonazoid in healthy volunteers and in patients with reduced pulmonary diffusing capacity. Ultrasound Med Biol. Mar; 2008 34(3):494–501. [PubMed: 18096304]
8. Sheeran PS, Dayton PA. Phase-change contrast agents for imaging and therapy. Current Pharmaceutical Design. May; 2012 18(15):2152–2165. [PubMed: 22352770]
9. Rapoport N. Phase-shift, stimuli-responsive perfluorocarbon nanodroplets for drug delivery to cancer. Wiley Interdiscip Rev Nanomed Nanobiotechnol. Sep; 2012 4(5):492–510. [PubMed: 22730185]
10. Lin C-Y, Pitt WG. Acoustic droplet vaporization in biology and medicine. BioMed Res Int. Oct. 2013 2013:1–13.
11. Evans DR, Parsons DF, Craig VS. Physical properties of phase-change emulsions. Langmuir. Oct; 2006 22(23):9538–9545. [PubMed: 17073477]
12. Kripfgans OD, Fowlkes JB, Miller DL, Eldevik OP, Carson PL. Acoustic droplet vaporization for therapeutic and diagnostic applications. Ultrasound Med Biol. Sep; 2000 26(7):1177–1189. [PubMed: 11053753]
13. Schad KC, Hynynen K. *In vitro* characterization of perfluorocarbon droplets for focused ultrasound therapy. Phys Med Biol. Aug; 2010 55(17):4933–4947. [PubMed: 20693614]
14. Shpak O, Verweij M, Vos HJ, de Jong N, Lohse D, Versluis M. Acoustic droplet vaporization is initiated by superharmonic focusing. Proc Nat Acad Sci USA. Jan; 2014 111(5):1697–1702. [PubMed: 24449879]

15. Prabhakar U, et al. Challenges and key considerations of the enhanced permeability and retention effect for nanomedicine drug delivery in oncology. Cancer Res. Apr; 2013 73(8):2412–2417. [PubMed: 23423979]
16. Rapoport NY, Kennedy AM, Shea JE, Scaife CL, Nam KH. Controlled and targeted tumor chemotherapy by ultrasound-activated nanoemulsions/microbubbles. J Controlled Release. Sep; 2009 138(3):268–276.
17. Sheeran PS, et al. Decafluorobutane as a phase-change contrast agent for low-energy extravascular ultrasonic imaging. Ultrasound Med Biol. Sep; 2011 37(9):1518–1530. [PubMed: 21775049]
18. Reznik N, Williams R, Burns PN. Investigation of vaporized submicron perfluorocarbon droplets as an ultrasound contrast agent. Ultrasound Med Biol. Aug; 2011 37(8):1271–1279. [PubMed: 21723449]
19. Zhang P, Porter T. An *in vitro* study of a phase-shift nanoemulsion: A potential nucleation agent for bubble-enhanced HIFU tumor ablation. Ultrasound Med Biol. Nov; 2010 36(11):1856–1866. [PubMed: 20888685]
20. Moyer LC, Timbie KF, Sheeran PS, Price RJ, Miller GW, Dayton PA. High-intensity focused ultrasound ablation enhancement *in vivo* via phase-shift nanodroplets compared to microbubbles. J Therapeutic Ultrasound. May; 2015 3(1):1–9.
21. Paproski RJ, Forbrich A, Hitt M, Zemp R. RNA biomarker release with ultrasound and phase-change nanodroplets. Ultrasound Med Biol. Aug; 2014 40(8):1847–1856. [PubMed: 24792584]
22. Sheeran PS, Streeter JE, Mullin LB, Matsunaga TO, Dayton PA. Toward ultrasound molecular imaging with phase-change contrast agents: An *in vitro* proof of principle. Ultrasound Med Biol. May; 2013 39(5):893–902. [PubMed: 23453380]
23. Sheeran PS, Rojas JD, Puett C, Hjelmquist J, Arena CB, Dayton PA. Contrast-enhanced ultrasound imaging and *in vivo* circulation kinetics with low boiling point nanoscale phase-change perfluorocarbon agents. Ultrasound Med Biol. Mar; 2015 41(3):814–831. [PubMed: 25619781]
24. Zhang M, et al. Acoustic droplet vaporization for enhancement of thermal ablation by high intensity focused ultrasound. Acad Radiol. Sep; 2011 18(9):1123–1132. [PubMed: 21703883]
25. Kasoji SK, et al. Cavitation enhancing nanodroplets mediate efficient DNA fragmentation in a bench top ultrasonic water bath. PLoS One. Jul; 2015 10(7):1–15.
26. Moncion A, et al. Design and characterization of fibrin-based acoustically responsive scaffolds for tissue engineering applications. Ultrasound Med Biol. Jan; 2016 42(1):257–271. [PubMed: 26526782]
27. Pitt WG, Singh RN, Perez KX, Husseini GA, Jack DR. Phase transitions of perfluorocarbon nanoemulsion induced with ultrasound: A mathematical model. Ultrason Sonochem. Mar; 2014 21(2):879–891. [PubMed: 24035720]
28. Mountford PA, Smith WS, Borden MA. Fluorocarbon nanodrops as acoustic temperature probes. Langmuir. Sep; 2015 31(39):10656–10663. [PubMed: 26359919]
29. Mountford PA, Thomas AN, Borden MA. Thermal activation of superheated lipid-coated perfluorocarbon drops. Langmuir. Apr; 2015 31(16):4627–4634. [PubMed: 25853278]
30. Kripfgans OD, Fabiilli ML, Carson PL, Fowlkes JB. On the acoustic vaporization of micrometer-sized droplets. J Acoust Soc Amer. Jul; 2004 116(1):272–281. [PubMed: 15295987]
31. Doinikov AA, Sheeran PS, Bouakaz A, Dayton PA. Vaporization dynamics of volatile perfluorocarbon droplets: A theoretical model and *in vitro* validation. Med Phys. 2014; 41(10): 102901. [PubMed: 25281982]
32. Shpak O, et al. Ultrafast dynamics of the acoustic vaporization of phase-change microdroplets. J Acoust Soc Amer. 2013; 134(2):1610–1621. [PubMed: 23927201]
33. Mountford PA, Sirsi SR, Borden MA. Condensation phase diagrams for lipid-coated perfluorobutane microbubbles. Langmuir. May; 2014 30(21):6209–6218. [PubMed: 24824162]
34. Eberhart JG. The thermodynamic and the kinetic limits of superheat of a liquid. J Colloid Interface Sci. Aug; 1976 56(2):262–269.
35. Sheeran PS, Yoo K, Williams R, Yin M, Foster FS, Burns PN. More than bubbles: Creating phase-shift droplets from commercially available ultrasound contrast agents. Ultrasound Med Biol. accepted for publication.

36. Miles CJ, Doering CR, Kripfgans OD. Nucleation pressure threshold in acoustic droplet vaporization. J Appl Phys. 2016; 120(3):034903.
37. Fabiilli ML, Haworth KJ, Fakhri NH, Kripfgans OD, Carson PL, Fowlkes JB. The role of inertial cavitation in acoustic droplet vaporization. IEEE Trans Ultrason, Ferroelectr, Freq Control. May; 2009 56(5):1006–1017. [PubMed: 19473917]
38. Sheeran PS, Luois SH, Mullin LB, Matsunaga TO, Dayton PA. Design of ultrasonically-activatable nanoparticles using low boiling point perfluorocarbons. Biomaterials. Apr; 2012 33(11):3262–3269. [PubMed: 22289265]
39. Dove JD, Mountford PA, Murray TW, Borden MA. Engineering optically triggered droplets for photoacoustic imaging and therapy. Biomed Opt Exp. Dec; 2014 5(12):4417–4427.
40. Riess JG. Understanding the fundamentals of perfluorocarbons and perfluorocarbon emulsions relevant to *in vivo* oxygen delivery. J Artificial Cells, Blood Substitutes, Biotechnol. Jul; 2005 33(1):47–63.
41. Kawabata K, Sugita N, Yoshikawa H, Azuma T, Umemura S. Nanoparticles with multiple perfluorocarbons for controllable ultrasonically induced phase shifting. Jpn J Appl Phys. Jun.2005 44(6B):5.
42. Martin AL, Seo M, Williams R, Belayneh G, Foster FS, Matsuura N. Intracellular growth of nanoscale perfluorocarbon droplets for enhanced ultrasound-induced phase-change conversion. Ultrasound Med Biol. Oct; 2012 38(10):1799–1810. [PubMed: 22920544]
43. Sheeran PS, et al. Image-guided ultrasound characterization of volatile sub-micron phase-shift droplets in the 20–40 MHz frequency range. Ultrasound Med Biol. Mar; 2016 42(3):795–807. [PubMed: 26725168]
44. Reznik N, et al. On the acoustic properties of vaporized submicron perfluorocarbon droplets. Ultrasound Med Biol. Jun; 2014 40(6):1379–1384. [PubMed: 24462162]
45. Reznik N, et al. The efficiency and stability of bubble formation by acoustic vaporization of submicron perfluorocarbon droplets. Ultrasonics. Sep; 2013 53(7):1368–1376. [PubMed: 23652262]
46. Hill ML, et al. Towards a nanoscale mammographic contrast agent: Development of a modular pre-clinical dual optical/x-ray agent. Phys Med Biol. Jul.2013 58(15):5215. [PubMed: 23851978]
47. Gorelikov I, Martin AL, Seo M, Matsuura N. Silica-coated quantum dots for optical evaluation of perfluorocarbon droplet interactions with cells. Langmuir. Oct; 2011 27(24):15024–15033. [PubMed: 22026433]
48. Xu H, Zeiger BW, Suslick KS. Sonochemical synthesis of nanomaterials. Chem Soc Rev. Nov; 2012 42(7):2555–2567.
49. Taurozzi JS, Hackley VA, Wiesner MR. Preparation of nanoparticle dispersions from powdered material using ultrasonic disruption. NIST Special Publication. Jun.2012 1200–2:1–14.
50. Kopechek JA, Zhang P, Burgess MT, Porter TM. Synthesis of phase-shift nanoemulsions with narrow size distributions for acoustic droplet vaporization and bubble-enhanced ultrasound-mediated ablation. J Vis Experiments. Sep.2012 13(67):e4308.
51. Strohm E, Rui M, Gorelikov I, Matsuura N, Kolios M. Vaporization of perfluorocarbon droplets using optical irradiation. Biomed Opt Exp. 2011; 2(6):1432–1442.
52. Strohm EM, Gorelikov I, Matsuura N, Kolios MC. Acoustic and photoacoustic characterization of micron-sized perfluorocarbon emulsions. J Biomed Opt. Sep; 2012 17(9):96016–96019. [PubMed: 23085917]
53. Strohm EM, Gorelikov I, Matsuura N, Kolios MC. Modeling photoacoustic spectral features of micron-sized particles. Phys Med Biol. Sep.2014 59(19):5795. [PubMed: 25207464]
54. Sheeran PS, Luois S, Dayton PA, Matsunaga TO. Formulation and acoustic studies of a new phase-shift agent for diagnostic and therapeutic ultrasound. Langmuir. Jul; 2011 27(17):10412–10420. [PubMed: 21744860]
55. Paproski RJ, et al. Porphyrin nanodroplets: Sub-micrometer ultrasound and photoacoustic contrast imaging agents. Small. Jan; 2016 12(3):371–380. [PubMed: 26633744]
56. Feshitan JA, Chen CC, Kwan JJ, Borden MA. Microbubble size isolation by differential centrifugation. J Colloid Interface Sci. Jan; 2009 329(2):316–324. [PubMed: 18950786]

57. Sheeran PS, Matsunaga TO, Dayton PA. Phase-transition thresholds and vaporization phenomena for ultrasound phase-change nanoemulsions assessed via high-speed optical microscopy. Phys Med Biol. Jun.2013 58(13):4513. [PubMed: 23760161]
58. Shpak O, Stricker L, Versluis M, Lohse D. The role of gas in ultrasonically driven vapor bubble growth. Phys Med Biol. Mar.2013 58(8):2523. [PubMed: 23528293]
59. Anna SL, Mayer HC. Microscale tipstreaming in a microfluidic flow focusing device. Phys Fluids. Dec.2006 18(12):121512.
60. Malloggi F, et al. Monodisperse colloids synthesized with nanofluidic technology. Langmuir. Nov; 2010 26(4):2369–2373. [PubMed: 19916489]
61. Couture O, et al. Ultrasound internal tattooing. Med Phys. Feb; 2011 38(2):1116–1123. [PubMed: 21452748]
62. Martz TD, Bardin D, Sheeran PS, Lee AP, Dayton PA. Microfluidic generation of acoustically active nanodroplets. Small. Jun; 2012 8(12):1876–1879. [PubMed: 22467628]
63. Christopher GF, Anna SL. Microfluidic methods for generating continuous droplet streams. J Phys D, Appl Phys. Sep.2007 40(19):R319.
64. Shui L, Berg A, Eijkel JCT. Scalable attoliter monodisperse droplet formation using multiphase nanomicrofluidics. Microfluidics Nanofluidics. Jul; 2011 11(1):87–92.
65. Seo M, Matsuura N. Direct incorporation of lipophilic nanoparticles into monodisperse perfluorocarbon nanodroplets via solvent dissolution from microfluidic-generated precursor microdroplets. Langmuir. Sep; 2014 30(42):12465–12473. [PubMed: 25188556]
66. Seo M, Zhu S, Matsuura N. Diethyl ether as a drug-loading and sizereducing cosolvent to produce monodisperse, nanoscale perfluoro-carbon agents. Proc IEEE Int Ultrason Symp (IUS). Oct.2015 : 1–4.
67. Seo M, Matsuura N. Monodisperse, submicrometer droplets via condensation of microfluidic-generated gas bubbles. Small. Sep; 2012 8(17):2704–2714. [PubMed: 22700364]
68. Seo M, Williams R, Matsuura N. Size reduction of cosolvent-infused microbubbles to form acoustically responsive monodisperse perfluorocarbon nanodroplets. Lab Chip. Jul; 2015 15(17): 3581–3590. [PubMed: 26220563]
69. Seo M, Gorelikov I, Williams R, Matsuura N. Microfluidic assembly of monodisperse, nanoparticle-incorporated perfluorocarbon microbubbles for medical imaging and therapy. Langmuir. Jul; 2010 26(17):13855–13860. [PubMed: 20666507]
70. Couture O, Bevan PD, Cherin E, Cheung K, Burns PN, Foster FS. Investigating perfluorohexane particles with high-frequency ultrasound. Ultrasound Med Biol. 2006; 32(1):73–82. [PubMed: 16364799]
71. Lanza GM, Wickline SA. Targeted ultrasonic contrast agents for molecular imaging and therapy. Prog Cardiovascular Diseases. 2001; 44(1):13–31.
72. Hackley VA, Clogston JD. Measuring the hydrodynamic size of nanoparticles in aqueous media using batch-mode dynamic light scattering. Methods Mol Biol. Oct.2011 697:35–52. [PubMed: 21116952]
73. Anderson W, Kozak D, Coleman VA, Jämting K, Trau M. A comparative study of submicron particle sizing platforms: Accuracy, precision and resolution analysis of polydisperse particle size distributions. J Colloid Interface Sci. Sep.2013 405:322–330. [PubMed: 23759321]
74. Filipe V, Hawe A, Jiskoot W. Critical evaluation of nanoparticle tracking analysis (NTA) by NanoSight for the measurement of nanoparticles and protein aggregates. Pharmaceutical Res. 2010; 27(5):796–810.
75. Asami R, Kawabata K. Repeatable vaporization of optically vaporizable perfluorocarbon droplets for photoacoustic contrast enhanced imaging. Proc IEEE Int Ultrason Symp (IUS). Oct.2012 : 1200–1203.
76. Kang ST, Huang YL, Yeh CK. Characterization of acoustic droplet vaporization for control of bubble generation under flow conditions. Ultrasound Med Biol. 2014; 40(3):551–561. [PubMed: 24433748]
77. Arnal B, et al. Sono-photoacoustic imaging of gold nanoemulsions: Part I. Exposure thresholds. Photoacoustics. 2015; 3(1):3–10. [PubMed: 25893169]

78. Li S, Lin S, Cheng Y, Matsunaga TO, Eckersley RJ, Tang MX. Quantifying activation of perfluorocarbon-based phase-change contrast agents using simultaneous acoustic and optical observation. Ultrasound Med Biol. Apr; 2015 41(5):1422–1431. [PubMed: 25656747]

79. Linstrom, PJ., Mallard, WG., editors. NIST Chemistry WebBook. National Institute of Standards and Technology; Gaithersburg, MD, USA: 2016. (NIST Standard Reference Database Number 69)

Biographies

Paul S. Sheeran (S'12–M'14) received the dual B.S. degrees in electrical and computer engineering from North Carolina State University, Raleigh, NC, USA, in 2007, and the Ph.D. degree from the Joint Biomedical Engineering Department, University of North Carolina and North Carolina State University, Chappel Hill, NC, USA, in 2014.

He is currently a Banting Postdoctoral Fellow with the Sunnybrook Research Institute, Toronto, ON, Canada. His current research interests include the design and characterization of ultrasound-activated contrast agents, development of ultrasound imaging sequences, and the therapeutic applications of ultrasound.

Naomi Matsuura is currently an Assistant Professor with the Department of Medical Imaging and Materials Science and Engineering, University of Toronto, Toronto, ON, Canada. Her current research interests include the design of new, translatable contrast agents to guide the personalized treatment of cancer for individual patients, with a particular interest in designing new materials that can interact specifically with medical imaging radiation for minimally-invasive, image-guided, and site-specific delivery of cancer therapies to tumors *In Vivo*.

Mark A. Borden (M'04) received the B.S. degree in chemical engineering from the University of Arizona, Tucson, AZ, USA, in 1999, and the Ph.D. degree in chemical engineering from the University of California at Davis (UC Davis), Davis, CA, USA, in 2003.

He was a Postdoctoral Researcher with Biomedical Engineering, UC Davis, and a Visiting Scientist in radiology with the Arizona Cancer Center, Scottsdale, AZ, USA. He was an Assistant Professor of Chemical Engineering with Columbia University, New York, NY, USA, from 2007 to 2010. Since 2010, he has been an Associate Professor of Mechanical Engineering with the University of Colorado, Boulder, CO, USA. His current research interests include the development of microbubbles and other soft colloids for applications in ultrasound molecular imaging, ultrasound-targeted drug, gene delivery, and injectable oxygen.

Ross Williams received the B.A.Sc. degree in engineering science from the University of Toronto, Toronto, ON, Canada, in 2002.

He is currently a Research Engineer with the Sunnybrook Research Institute, Toronto. His current research interests include the characterization and application of ultrasound contrast agents.

Terry O. Matsunaga received the B.A. degree in biochemistry from the University of California at Berkeley, Berkeley, CA, USA, and the Pharm.D. and Ph.D. degrees from the University of California at San Francisco, San Francisco, CA, USA.

He was a Postdoctoral Fellow with the Department of Chemistry, University of Arizona, Tucson, AZ, USA. He was a Vice President for research with ImaRx Pharmaceutical and ImaRx Therapeutics (Tucson, AZ), where he was involved in the basic and regulatory development of microbubble contrast agents. Since 2007, he has been with the University of Arizona, where he is currently a Research Professor of Medical Imaging. His current

research interests include the development of ultrasound contrast agents for imaging and therapy.

Peter N. Burns was born in the U.K.. He received First Class Honours in theoretical physics. He studied philosophy of science before receiving the Ph.D. degree in radiodiagnosis from the University of Bristol, Bristol, UK.

In 1984, he was an Assistant Professor of Radiology with Yale University, New Haven, CT, USA. He then spent four years with the Department of Diagnostic Radiology, Thomas Jefferson University, Philadelphia, PA, USA, before moving to Canada in 1991. He is currently a Professor and the Chair of Medical Biophysics with the University of Toronto, Toronto, ON, Canada, and a Senior Scientist with the Sunnybrook Health Sciences Center, Toronto. He is involved in color Doppler instrumentation and hemodynamic measurement with Doppler and ultrasound contrast agents. His current research interests include blood flow detection and instrumentation for Doppler ultrasound, where he was a part of the early efforts to detect blood flow in tumors and other small vessel systems.

Paul A. Dayton (S’98–M’01) received the B.S. degree in physics from Villanova University, Villanova, PA, USA, in 1995, and the M.E. degree in electrical engineering and the Ph.D. degree in biomedical engineering from the University of Virginia, Charlottesville, VA, USA, in 1998 and 2001, respectively.

He was a Postdoctoral Researcher and later a Research Faculty Member with the University of California at Davis, Davis, CA, USA. Much of his training was under the mentorship of Dr. K. Ferrara; his initial studies involved the high speed optical and acoustical analysis of individual contrast agent microbubbles. Since 2007, he has been with the Joint Department of Biomedical Engineering, University of North Carolina at Chapel Hill, Chapel Hill, NC, USA, and North Carolina State University, Raleigh, NC, USA, where he is currently a Professor and the Associate Department Chair. He is also an Associate Director for Education with the Biomedical Imaging Research Center. His current research interests include ultrasound contrast imaging, ultrasound-mediated therapies, and medical devices.

Dr. Dayton is a member of the Technical Program Committee for the IEEE UFFC, and a member of the editorial boards for the journals IEEE Transactions on Ultrasonics, Ferroelectrics, and Frequency Control as well as *Molecular Imaging*, and *Bubble Science, Engineering, and Technology*.

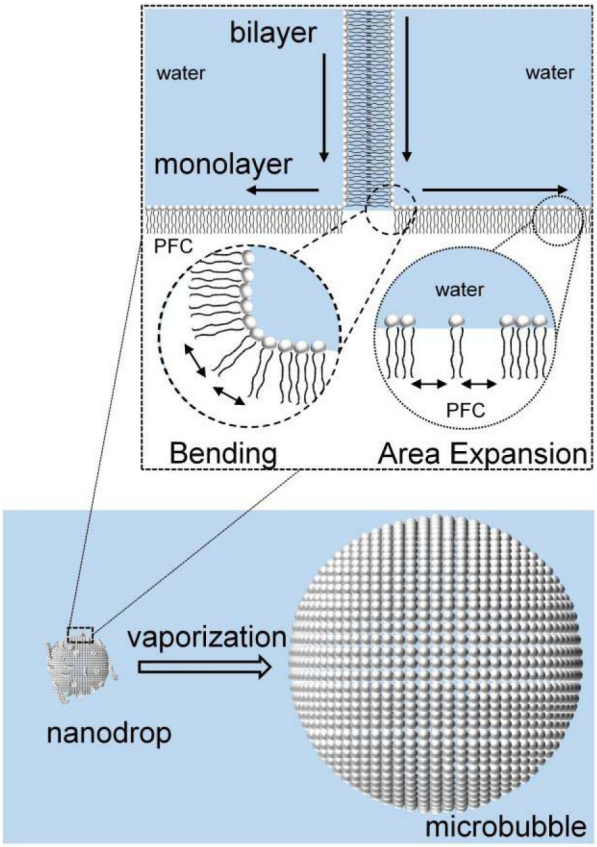

Fig. 1.

For lipid encapsulations, droplet-to-microbubble vaporization requires rapid spreading of lipid at the gas/water interface to accommodate the area expansion. The elastic cohesion energy would resist both monolayer expansion and leaflet bending from the unfolding of surface-attached bilayers, and thus the cohesion energy may add to the overall energy barrier for vaporization. Reproduced with permission from [29]. Copyright 2015 American Chemical Society.

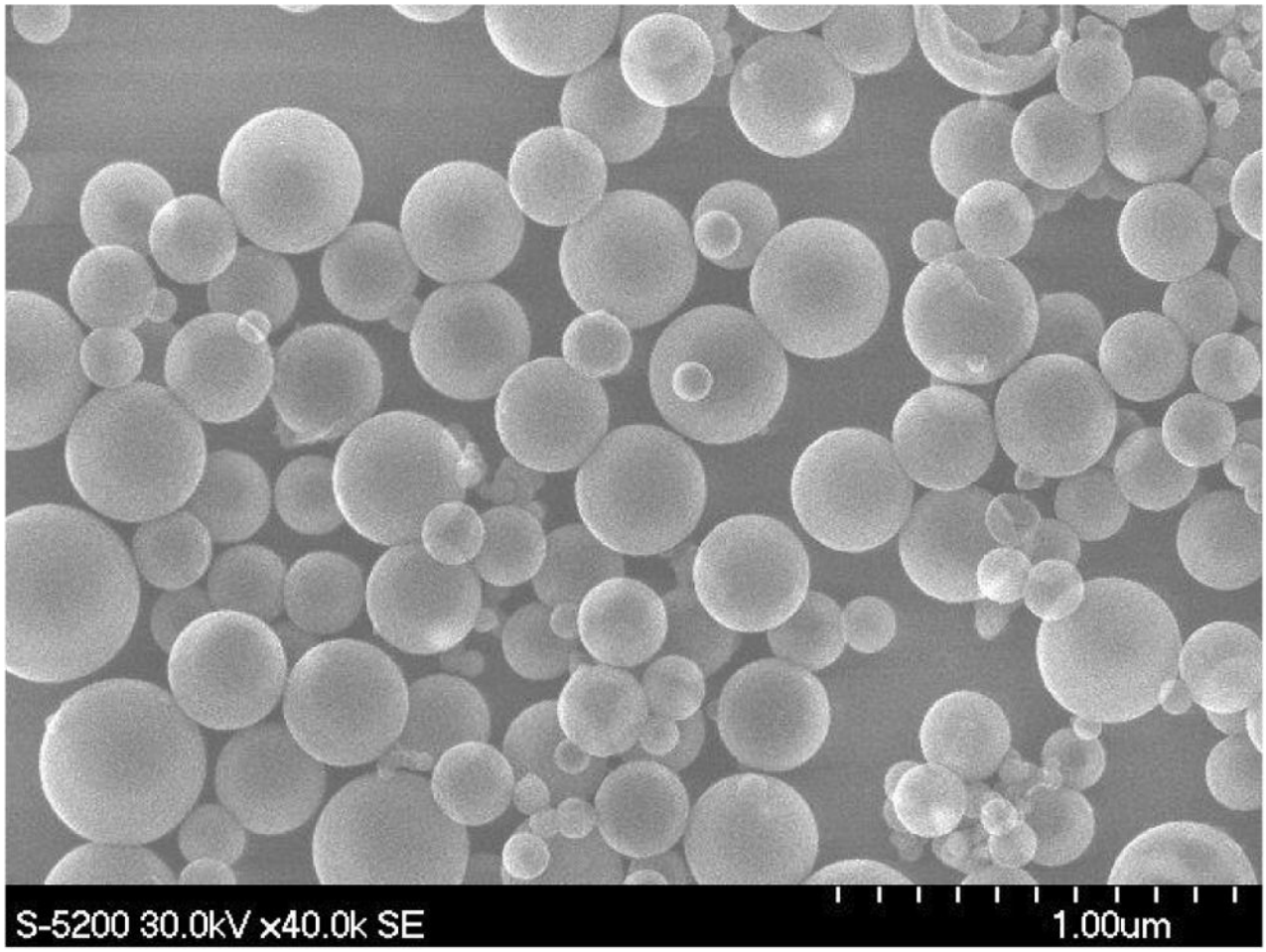

Fig. 2.

Example of polydisperse size distribution of tip-sonicated PFC droplets. Here PFH droplets were templated with silica in order to image them effectively using scanning electron microscopy.

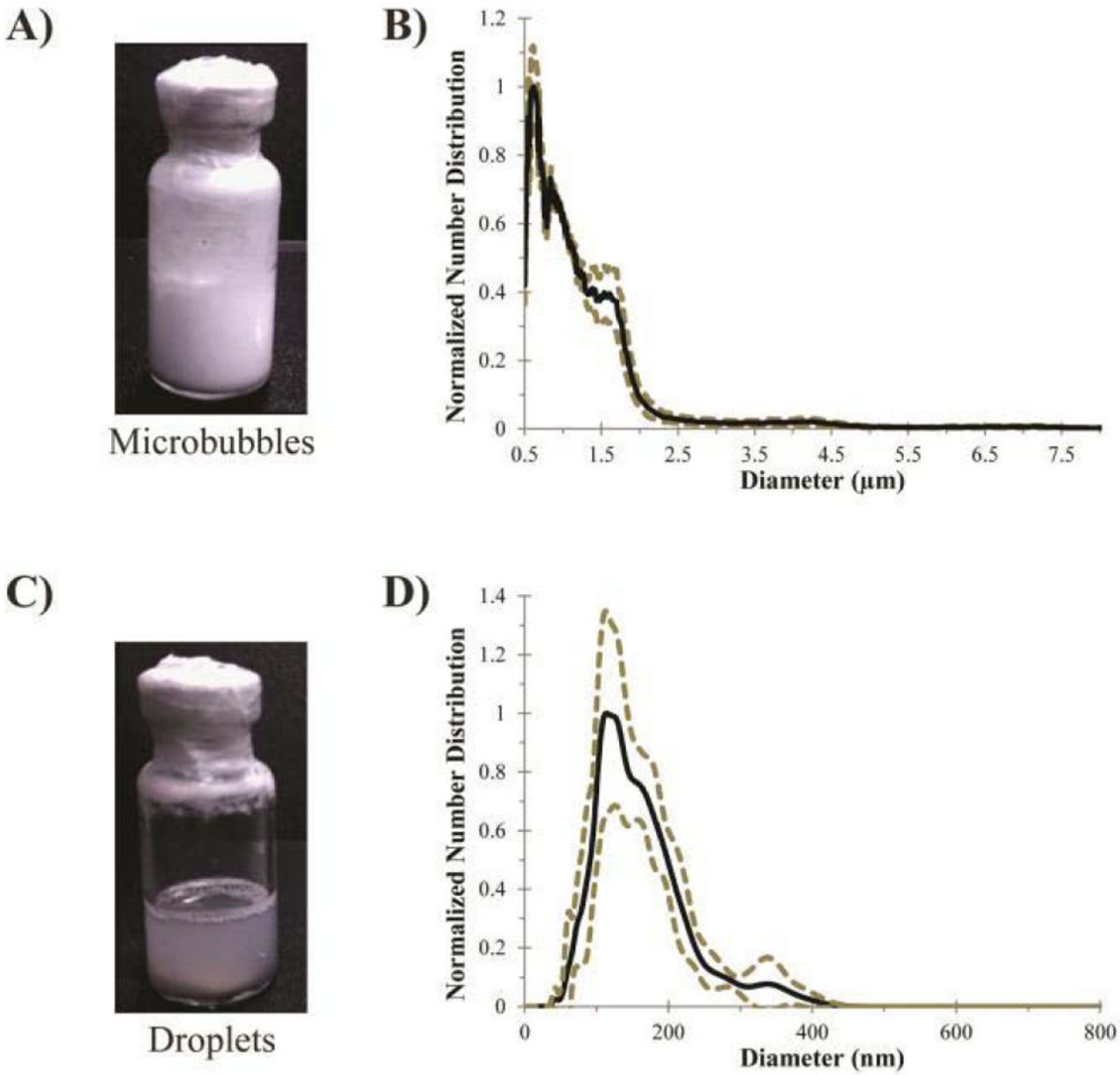

Fig. 3.

Microbubble condensation to form submicrometer droplets from volatile compounds (from [23]). (a) Phospholipid-encapsulated DFB microbubbles initially appear as an opaque "milky" emulsion. (b) Produce a distribution with a mean diameter of 1.0 ± 0.9 μm (N = 3, Accusizer 780, five-point smoothing applied). (c) After condensation, the emulsion appearance turns translucent. (d) Distribution shifts into the nanoscale with a mean diameter of 164 ± 63 μm (N = 3, Malvern NS-500). Dashed lines represent one standard deviation.

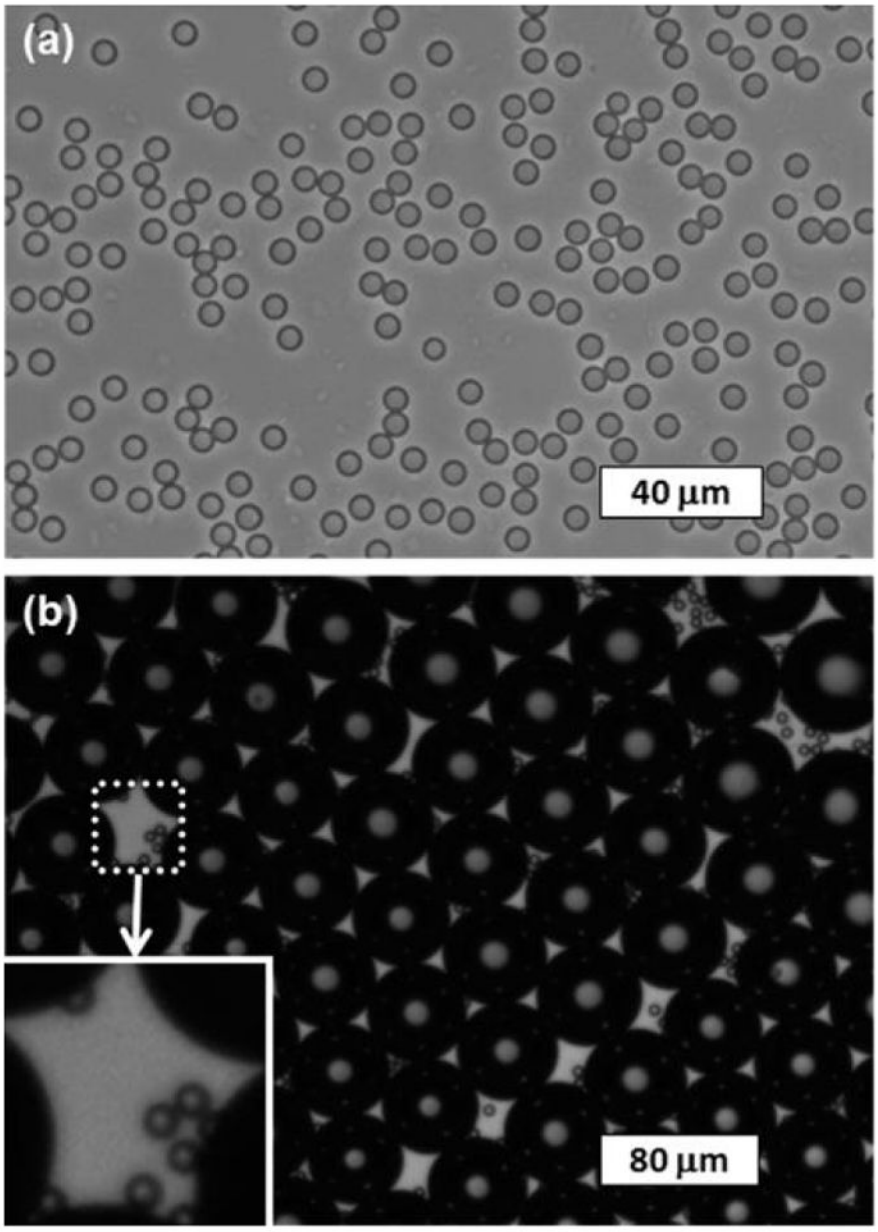

Fig. 4.

Example of monodisperse DDFP droplets before and after conversion into bubbles. (a) Microscope image of droplets (mean diameter = 6.6 μm and CV = 2.7%) on the glass slide after complete condensation and cosolvent dissolution from the precursor cosolvent-infused bubbles. (b) Microscope images of droplets and bubbles (mean diameter = 52.4 μm and CV = 3.5%) embedded in PAA gel after exposure to high-pressure ultrasound, showing the monodispersity of both the converted bubbles and the unconverted droplets (shown in the white inset box). The image was taken 4 min after high-pressure ultrasound exposure. Reproduced from [68] with permission from The Royal Society of Chemistry.

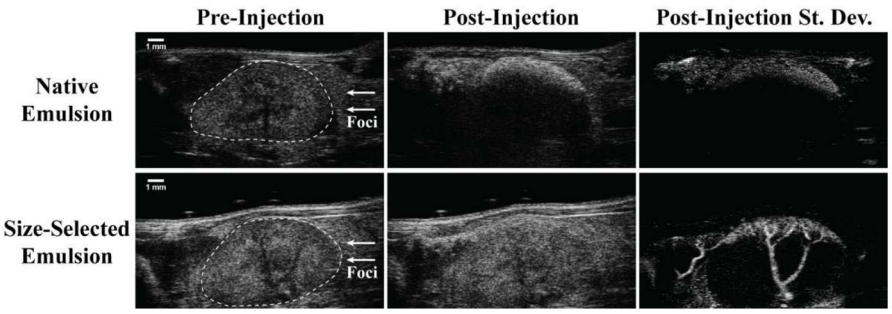

Fig. 5.

Visualization of DFB droplet vaporization within the mouse kidney at 30-MHz nominal center frequency with a standard B-mode imaging sequence. Here, two droplet emulsions prepared by microbubble condensation are compared. Each produces a DLS measurement with a peak in the 200–300-nm range, but the “size-selected emulsion” has been processed to remove large outliers not represented by DLS [43]. When exposed to 100% power 5 min after injection, bubble formation was observed in the proximal kidney cortex. Native emulsions resulted in a high degree of stationary contrast in the cortex with significant shadowing deep in the kidney—indicative of occlusion by large bubbles produced from outlier droplets, whereas size-selected emulsions produced primarily free-flowing bubbles of lower echogenicity that appeared as speckle variance from frame to frame. Passing the B-mode cine loops through a standard deviation filter, removing frames containing breathing motion, and summing the remaining frames illustrates the significant qualitative differences between the two emulsions, with size-selected droplets producing significantly greater speckle variance along the kidney cortex and through the associated interlobar veins. *Note*: hand-drawn ROI added to preinjection B-mode images in order to delineate kidney boundaries from surrounding tissue. Reproduced from [43] with permission from Elsevier.

TABLE I

Perfluorocarbon Properties

Chemical Formula	Name	Molecular Weight (g/mol)	Boiling Point (°C)	Approximate Limit of Superheat (~90% Critical Temperature) (°C)
C_6F_{14}	Perfluorohexane (PFH)	338	59	131
C_5F_{12}	Dodecafluoropentane (DDFP)	288	29	107
C_4F_{10}	Decafluorobutane (DFB)	238	−2	75
C_3F_8	Octafluoropropane (OFP)	188	−37	37

Values reproduced from [29], [79].